Journal of Electron Spectroscopy and Related Phenomena 198 (2015) 6–11

Contents lists available at ScienceDirect

Journal of Electron Spectroscopy and Related Phenomena

journal homepage: www.elsevier.com/locate/elspec

Polarization dependent hard X-ray photoemission experiments for solids: Efficiency and limits for unraveling the orbital character of the valence band

J. Weinen[a,*], T.C. Koethe[b], C.F. Chang[a], S. Agrestini[a], D. Kasinathan[a], Y.F. Liao[c], H. Fujiwara[b,1], C. Schüßler-Langeheine[b,2], F. Strigari[b], T. Haupricht[b], G. Panaccione[d], F. Offi[e], G. Monaco[f,3], S. Huotari[f,4], K.-D. Tsuei[c], L.H. Tjeng[a,b]

[a] Max Planck Institute for Chemical Physics of Solids, Nöthnitzer Str. 40, 01187 Dresden, Germany
[b] II. Physikalisches Institut, Universität zu Köln, Zülpicher Straße 77, 50937 Köln, Germany
[c] National Synchrotron Radiation Research Center, 101 Hsin-Ann Road, Hsinchu Science-Park, Hsinchu 30077, Taiwan
[d] TASC Laboratory, IOM-CNR, Area Science Park, S.S.14, Km 163.5, I-34149 Trieste, Italy
[e] CNISM and Dipartimento di Scienze, Università Roma Tre, Via della Vasca Navale 84, I-00146 Rome, Italy
[f] European Synchrotron Radiation Facility, BP220, 38043 Grenoble, France

ARTICLE INFO

Article history:
Received 7 August 2014
Received in revised form 4 November 2014
Accepted 10 November 2014
Available online 18 November 2014

PACS:
79.60.−i
71.20.−b
71.27.+a

Keywords:
Hard X-ray photoemission
Correlated materials
Electronic structure
Chemical bonding
Photoionization cross section
Photoelectron angular distribution

ABSTRACT

We have investigated the efficiency and limits of polarization dependent hard X-ray photoelectron spectroscopy (HAXPES) in order to establish how well this method can be used to unravel quantitatively the contributions of the orbitals forming the valence band of solids. By rotating the energy analyzer rather than the polarization vector of the light using a phase retarder, we obtained the advantage that the full polarization of the light is available for the investigation. Using NiO, ZnO, and Cu_2O as examples for solid state materials, we established that the polarization dependence is much larger than in photoemission experiments utilizing ultra-violet or soft X-ray light. Yet we also have discovered that the polarization dependence is less than complete on the basis of atomic calculations, strongly suggesting that the trajectories of the outgoing electrons are affected by appreciable side-scattering processes even at these high kinetic energies. We have found in our experiment that these can be effectively described as a directional spread of ±18° of the photoelectrons. This knowledge allows us to identify, for example, reliably the Ni 3*d* spectral weight of the NiO valence band and at the same time to demonstrate the importance of the Ni 4*s* for the chemical stability of the compound.

1. Introduction

With bulk sensitivity being an important characteristic of HAXPES, another useful aspect of this technique appears to be the very pronounced dependence of the spectra on the polarization of the light. The selection rules in the photoexcitation process of electrons with linearly polarized light can in principle be used to identify the character of the orbitals contributing to the valence band [1–4]. Yet, transport of the photoelectrons to the surface and subsequent escape of the surface to the detector, involves scattering events that affect their angular intensity distributions. If the influence of these scattering processes can be estimated and the resulting effective polarization dependence can be made quantitative, one can obtain a very detailed understanding of the electronic structure of the material under study, especially when guided by theoretical

* Corresponding author. +49 351 4646 4901.
E-mail address: Jonas.Weinen@cpfs.mpg.de (J. Weinen).
[1] Present address: Graduate School of Engineering Science, Osaka University, 1-3 Machikaneyama, Toyonaka, Osaka 560-8531, Japan.
[2] Present address: Helmholtz-Zentrum Berlin für Materialien und Energie: Methods and Instrumentation in Synchrotron Radiation Research, Albert-Einstein-Str. 15, 12489 Berlin, Germany.
[3] Present address: Physics Department, University of Trento, Via Sommarive 14, 38123 Povo TN, Italy.
[4] Present address: Department of Physics, University of Helsinki, FI-00014, Finland.

http://dx.doi.org/10.1016/j.elspec.2014.11.003
0368-2048/

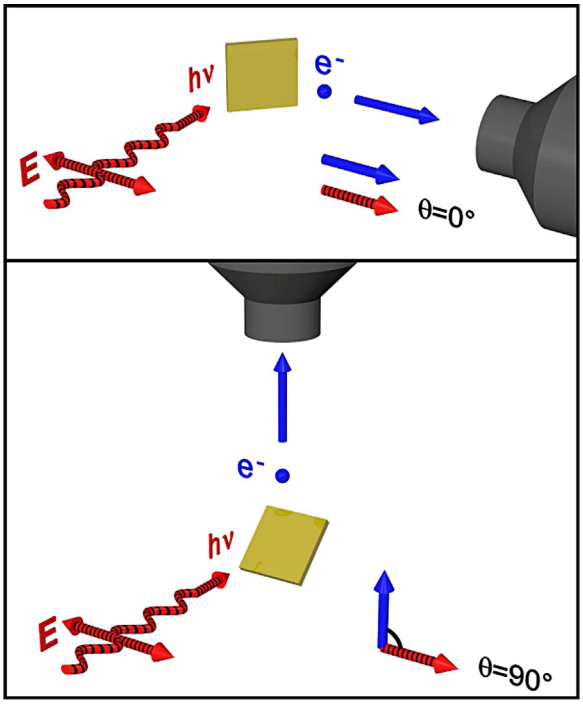

Fig. 1. Experimental geometry for different angles θ between the photon beam electrical field vector **E** (red, striped) and the momentum of the analyzed photoelectrons (blue). **E** is always horizontal, in the plane of the synchrotron storage ring. Top: analyzer mounted horizontally and parallel to the **E** vector, $\theta = 0^\circ$. Bottom: analyzer mounted vertically and perpendicular to **E**, $\theta = 90^\circ$. (For interpretation of the references to colour in this figure legend, the reader is referred to the web version of this article.)

ab-initio calculations. The polarization dependent HAXPES experiments reported so far [1–4] made use of phase retarders to rotate the polarization of the light. The efficiency of the retarders to generate vertically polarized light, however, is about 0.8 only [1–4]. This hampers a reliable determination of the limits of polarization dependent HAXPES due to the inaccuracies in the characterization of the efficiency of the phase retarders.

Here we followed a different route: instead of rotating the polarization of the light, we altered the position of the electron energy analyzer, i.e. we used three different experimental geometries: in the first geometry the analyzer is placed in the direction of the linear polarization of the light, in the second perpendicular to the light polarization, and in the third at 45° [5]. This experimental set-up has the advantage that all the spectra can be taken with the full light polarization provided by the undulator beam line. We have carried out experiments on NiO, ZnO and Cu_2O as model systems for transition metal oxides. We measured the transition metal 2*p* and O 1*s* core levels, as well as the valence band of NiO.

2. Experimental

The experiments have been carried out at the Max-Planck-NSRRC HAXPES station at the Taiwan undulator beamline BL12XU at SPring-8, Japan, and at the VOLPE station placed at beamline ID16 of the ESRF in Grenoble, France [6]. The photon beam is linearly polarized with the electrical field vector in the plane of the storage ring (i.e. horizontal). Photon energies of about 6.5 keV and 7.7 keV have been used.

In the first geometry, the analyzer (MB Scientific A-1 HE) was mounted horizontally and parallel to the photon beam's electrical field vector. See top panel of Fig. 1. The maximum angular acceptance was limited to ±15.3° (30.5° total acceptance) by the circular opening of the first lens element. In the second

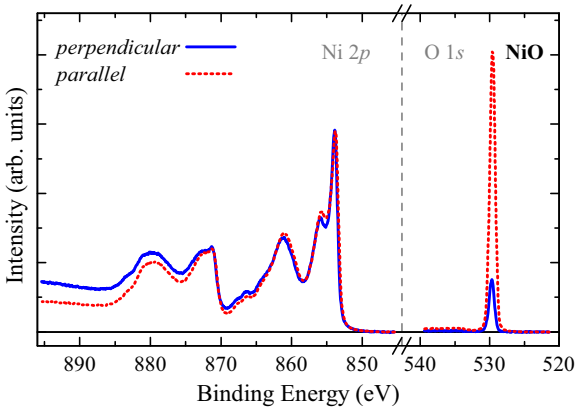

Fig. 2. HAXPES (photon energy 6.5 keV) spectra of NiO Ni 2*p* and O 1*s* core levels with $\theta = 90^\circ$ (perpendicular) and $\theta = 0^\circ$ (parallel).

geometry, the analyzer (MB Scientific A-1 HE) was mounted vertically, i.e. perpendicular to the electrical field vector and the Poynting vector of the beam. See bottom panel of Fig. 1. The maximum angular acceptance was limited to ±8.3° (16.6° total acceptance) by the circular opening of the first lens element. We have also utilized a third geometry, in which the analyzer (VOLPE/MB Scientific [6]) was put in the horizontal plane at 45° with respect to the electric field vector. A description of this is given in Ref. [5].

A NiO and a ZnO single crystal from SurfaceNet, Germany, were used. The Cu_2O sample was prepared by annealing a flat piece of oxidized copper metal in vacuum at 300° C [7]. All samples were measured at room temperature in a near normal emission geometry.

We have also performed X-ray photoemission (XPS) measurements for the NiO valence band using a Scienta SES-100 electron energy analyzer and a Vacuum Generators twin crystal monochromatized Al-K_α $h\nu = 1486.6$ eV source. The NiO single crystal was cleaved in-situ to obtain a clean surface.

3. Core levels

Fig. 2 displays the HAXPES Ni 2*p* and O 1*s* core level spectra of NiO taken with the photoelectron momentum parallel (red curves, $\theta = 0^\circ$) and perpendicular (blue curves, $\theta = 90^\circ$) to the polarization vector of the light. The photon energy was set at 6.5 keV and the overall energy resolution was 0.35–0.40 eV. The parallel vs. perpendicular spectra are normalized with respect to the Ni 2*p* main peak intensity. No corrections have been made to the spectra apart from a constant background subtraction. The line shape of the Ni 2*p* spectra is essentially identical to the ones published using also lower photon energies [8–13]. The O 1*s* spectrum shows a narrow single line demonstrating that the NiO sample is clean and of good quality. The relevant information that is contained in Fig. 2 is that the O 1*s* intensity is much lower for the perpendicular (blue curve) than for the parallel (red curve) polarization. This is qualitatively in agreement with the observations for *s*-orbitals in experiments in which the polarization has been varied using a phase retarder [1–4].

Making use of the fact that the degree of the photon polarization is identical for the two experimental geometries, we now can be quantitative concerning the physics underlying the change of the O 1*s* intensity with the photoelectron momentum. The expression for the angular dependence for the differential photoionization cross section is given by [14,15]

$$\frac{d\sigma}{d\Omega} = \frac{\sigma}{4\pi}\left[1 + \beta P_2(\cos\theta) + (\gamma\cos^2\theta + \delta)\sin\theta\cos\varphi\right] \quad (1)$$

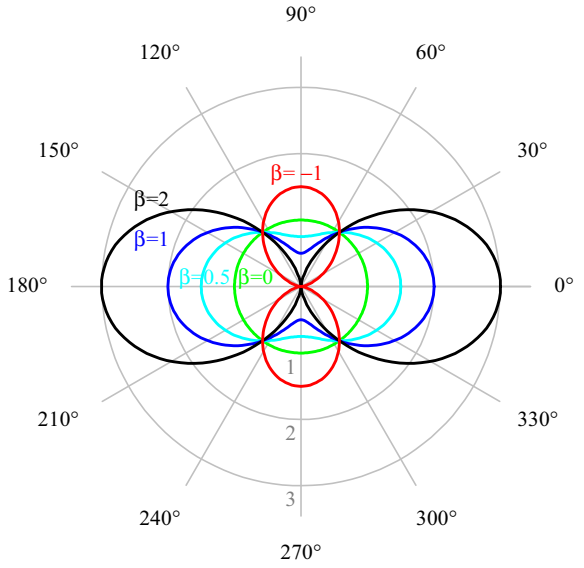

Fig. 3. Polar plot of the cross section angular dependence for various values of β.

where σ is the subshell photoionization cross section and P_2 the second Legendre polynomial. θ is the angle between the photoelectron momentum and the polarization vector of the light **E**, φ the angle between the photon momentum vector and the projection of the photoelectron momentum vector on the plane perpendicular to the electrical field vector and containing the photon momentum vector [16]. This corresponds to a spherical coordinate system with **E** in the z axis and the photon propagation in the x axis and where θ is the polar and φ the azimuthal angle. β, γ, and δ are the angular distribution parameters. The first two summands in Eq. (1) represent a dipolar approximation, the third summand includes non-dipolar effects. We have for the parallel geometry, i.e. with the analyzer along the electric field vector, $\theta = 0°$ (φ undefined) and for the perpendicular geometry $\theta = 90°$ and $\varphi = 90°$. The expression Eq. (1) now simplifies to

$$\frac{d\sigma}{d\Omega} = \frac{\sigma}{4\pi}\left\{1 + \beta\left(\frac{1}{4} + \frac{3}{4}\cos 2\theta\right)\right\}. \quad (2)$$

A polar plot of this angular dependence is shown in Fig. 3 for several values of β.

Ideally, in the atomic limit, β is 2 for s orbitals, so that for the perpendicular orientation, i.e. $\theta = 90°$, the intensity for the O 1s spectrum is expected to be zero. This is clearly not the case. Normalized to the Ni 2p intensities, the intensity ratio of the O 1s signal taken with perpendicular and parallel orientation is 0.16. Cross-section calculations for atomic orbitals provide a β value of about 0.98 for Ni 2p at $h\nu = 6.5$ keV [14,15] (angular distribution parameters are interpolated from tabulated values), so that the Ni 2p intensity ratio for perpendicular vs. parallel orientation should be close to 0.258 using Eq. (2). The real experimental O 1s intensity ratio is therefore $0.16 \times 0.258 = 0.041$. This is substantially larger (by a factor of ~5) than the expected value of 0.008 using Eq. (2) for the interpolated β value of about 1.952 for O 1s at $h\nu = 6.5$ keV [14,15].

To identify the origin of this discrepancy we will first investigate the effect of the acceptance angle of the electron energy analyzers. We first of all note that the third term in the sum in Eq. (1) still can be omitted for the two geometries used in our experiment when we consider the effect of the acceptance angles: for the parallel geometry, the acceptance angle in both the analyzer entrance slit and energy dispersive directions enters as variations of the θ angle symmetrically around $\theta = 0$, and will not integrate a non-zero value for the third term since $\sin\theta$ is an odd function of θ. For the perpendicular geometry, the acceptance angle in the analyzer entrance slit direction enters as variations in the φ angle symmetrically around $\varphi = 90°$. Since $\cos\varphi$ is an odd function around $\varphi = 90°$, the third term will not show up. The acceptance angle in the energy dispersive direction then also becomes irrelevant. We still can therefore use the simpler Eq. (2).

For both geometries, an analyzer entrance slit/aperture set was used which limited the angular acceptance in the energy dispersive direction to ±1.65°. Applying the Helmholtz–Lagrange relation [17], this corresponds to an acceptance of about ±3.5° at the lens entrance. The acceptance angle in the direction parallel to the analyzer entrance slit (i.e. perpendicular to the energy dispersive direction) is determined by the circular opening of the first element as specified above.

In order to calculate the cross-section average over the acceptance angle, we integrate Eq. (2) from $\theta - \alpha$ to $\theta + \alpha$ and divide by 2α, where $\pm\alpha$ denotes the acceptance angle. We arrive at:

$$\frac{d\sigma}{d\Omega} = \frac{\sigma}{4\pi}\left\{1 + \beta\left(\frac{1}{4} + \frac{3}{4}\cos 2\theta\frac{\sin 2\alpha}{2\alpha}\right)\right\} \quad (3)$$

The relevant acceptance angle for the parallel geometry is determined essentially by the acceptance along the analyzer entrance slit direction, i.e. ±15.3°, since this is much larger than the acceptance along the energy dispersive direction, i.e. ±3.5°. For the perpendicular geometry on the other hand, the acceptance along the analyzer entrance slit direction does not alter θ, so the relevant number here is the acceptance along the energy dispersive direction, i.e. ±3.5°. Using these numbers and Eq. (3), we have a theoretical Ni 2p intensity ratio for perpendicular vs. parallel orientation of 0.264 and 0.01 for the O 1s. The real experimental O 1s intensity ratio is $0.16 \times 0.264 = 0.042$. Clearly, this is much larger than expected on the basis of the cross-section tables including the effect of the analyzer acceptance angles (by a factor of ~5). In fact, in order to obtain a value of 0.042 we need for the analyzer in the perpendicular geometry acceptance angles of the order of ±18°, which is physically not possible with the ±8.3° acceptance dictated by the opening of the first lens. Apparently, we have to conclude that the acceptance angles of the analyzer do not form the limiting factor for the suppression of the O 1s signal in the perpendicular orientation.

To verify that the above described results are not singular, we also have performed measurements on other compounds, namely ZnO and Cu_2O. We even have used another experimental geometry [5]. Yet the results are very similar: we find that the experimental intensity ratio of the O 1s signal is larger by a factor of 4–5 than expected on the basis of the cross-section tables [5]. We therefore can safely conclude that this deviation from the atomic polarization dependence is not limited to NiO.

A possible explanation for this can perhaps be found in the (quasi-elastic) scattering processes which take place following the creation of the photoelectron [18–21]. Although forward scattering will be dominant at high kinetic energies, a non-negligible amount of side scattering processes will make it possible to change the propagation direction of part of the photoelectrons such that they enter the analyzer which they otherwise will not be able to do. The effective acceptance angle of the order of ±18° that we would need, as mentioned above, reflects this process [22]. We note that experiments using 700 eV photons did not reveal any significant polarization dependence for the O 1s [23], supporting the explanation on the basis of such scattering processes: the kinetic energy of the photoelectrons (ca. 170 eV) is so low, that side or even back scattering events dominate, leading to an almost complete loss of the relationship between the propagation direction of the photoelectron upon creation and the direction of the photoelectron when it enters the analyzer.

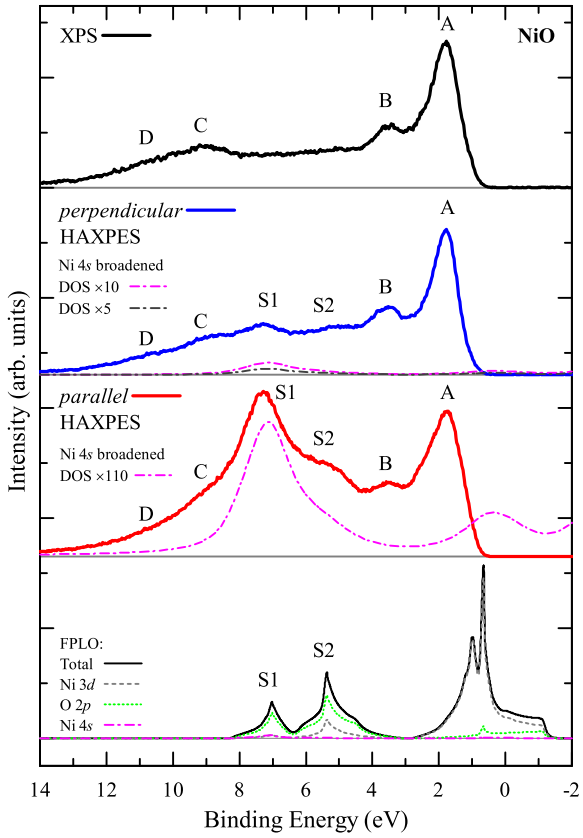

Fig. 4. XPS (photon energy 1.486 keV) and HAXPES (6.5 keV) spectra of NiO valence band with $\theta = 90^\circ$ (perpendicular) and $\theta = 0^\circ$ (parallel). LDA total and partial density of states from FPLO band structure calculations.

4. Valence band

In order to investigate to what extent these findings also affect HAXPES experiments on the valence band and especially the quantitative analysis of their polarization dependence, we also set out to collect the valence band spectrum of NiO. Fig. 4 displays the HAXPES spectrum taken with the perpendicular (second panel, blue curve) and parallel (third panel, red curve) geometries, together with the spectrum taken with the standard XPS using monochromatized $h\nu = 1486.6$ eV photons, as reference. The overall energy resolution of the XPS was set to 0.35 eV, as determined using the Fermi cutoff of a silver reference.

Starting with the XPS, we would like to note that this spectrum is very similar to the ones reported earlier in the literature [24–26] and that it shows the characteristic features labeled as A, B, C, and D, which are all related to the multiplet structure of the Ni 3*d* spectral weight [24–26]. The HAXPES spectra, interestingly, have different lineshapes with clear extra features labeled S1 and S2. In the perpendicular geometry, the intensities of these extra features are modest, but in the parallel geometry, the features dominate the spectrum.

To identify the origin of the S1 and S2 structures, we have performed LDA band structure calculations using the full-potential code with the basis set of local atomic-like orbitals (FPLO) [27]. The resulting total and partial densities of states (DOS) are depicted in the bottom panel of Fig. 4. Of particular interest is the Ni 4*s* partial DOS. We can clearly observe that the peak positions of the Ni 4*s* and O 2*p* bands coincide very well with structures S1 and S2. Indeed, looking at the tables [14,15], the ratio of the subshell photoionization cross section of the Ni 4*s* relative to that of the Ni 3*d* increases from 0.12 at $h\nu = 1486.6$ eV, to 0.99 at $h\nu = 5$ keV, and to 3.61 at $h\nu = 10$ keV, meaning that the contribution of the Ni 4*s* to the spectrum is negligible in XPS and that it becomes significant in the HAXPES experiment. The finding that HAXPES is much more sensitive to valence *s* orbitals is consistent with earlier reports and has been used to identify the partial density of states of the *s* orbital in semiconductors and metals [28–33].

This result in fact shows that HAXPES unveils an important part of the chemical bonding between the Ni and the O in the formation of NiO, namely the hybridization between the Ni 4*s* conduction band and the O 2*p* valence band. This provides an extra energy gain on top of the bonding energy due to the Ni 3*d* and O 2*p* hybridization. This Ni 4*s*–O 2*p* hybridization is analogous to that of Mg 3*s* and O 2*p* in MgO [34,35]. We would like to note that it is rather surprising that the LDA calculation can explain so well the experimentally observed structure S1. It is well known that due to the strongly correlated nature of the Ni 3*d* electrons the description of the electronic structure by theory is still a great challenge. Features A, B, C, and D require an explanation that includes at least aspects of configuration interaction and atomic multiplet effects [24–26]. The Ni 3*d* states and their hybridization with the O 2*p* will therefore result in an O 2*p* spectral weight that may be significantly different from the LDA O 2*p* partial DOS. The Ni 4*s* that couples to this O 2*p* may consequently show spectral weight at quite different energies than predicted by the LDA. It is therefore invaluable that the Ni 4*s* states can indeed be made visible experimentally. From the fact that the LDA does give a reasonable match to the experiment for the Ni 4*s* we can apparently deduce that the O 2*p* states that hybridize with the Ni 4*s* have a rather weak mixing with the Ni 3*d*. In hindsight, we may indeed see a justification for this in the form of a rather small Ni 3*d* and very high O 2*p* partial DOS in the LDA band that form the S1 structure.

We now analyze quantitatively the polarization dependence of the Ni 4*s* contribution to the spectrum. With the spectra normalized to the Ni 3*d* peak height at 2 eV binding energy, i.e. peak A, in the experiment and normalized to the Ni 3*d* peak height at 1 eV binding energy in the calculation, we can make an estimate for the relative contribution of the Ni 4*s* to the spectra. After broadening the calculated DOS with a 0.35 eV Gaussian to account for the experimental resolution and 1.9 eV Lorentzian for the life time (full width at half maximum values), we find for the parallel geometry that a multiplication by a factor of approximately 110 of the Ni 4*s* DOS gives a reasonable match for the intensity of structure S1. For the perpendicular geometry, we determine that a multiplication factor between approximately 5 and 10 is needed. Here the uncertainty is rather large due to the uncertainty in the estimate that one has to make for the background which is given primarily by the Ni 3*d* spectral weight. From the cross section tables we expect the Ni 3*d* to have an intensity ratio for perpendicular vs. parallel orientation of about 0.58. Here we make use of Eq. (3), with $\beta = 0.39$ for Ni 3*d* at $h\nu = 6.5$ keV [14,15,22]. The effect of the analyzer acceptance angle is included. We then find experimentally that the ratio for the Ni 4*s* polarization dependence is given by $5\text{–}10/110 \times 0.58 = 0.026\text{–}0.053$. This is again a very large contrast which demonstrates the power of polarization dependence to identify the contribution of *s* orbitals to the valence band. Using the polarization dependence rather than the photon energy dependence of the photoionization cross section has the advantage that one does not also vary the probing depth as is the case when comparing HAXPES with XPS.

Yet, on the basis of atomic cross-section calculation, we expect even a larger contrast, namely a Ni 4*s* intensity ratio of about 0.004 with $\beta = 1.984$ for Ni 4*s* [14,15]. Although the Ni 4*s* as defined in the LDA calculation using the FPLO code is not identical to that in the atomic Ni 4*s* cross-section calculation, we nevertheless can safely conclude that the reduction of the Ni 4*s* is in effect much less than can be expected on the basis of the atomic calculations including

the effect of the analyzer acceptance angles (by a factor of 6.5–13.3). This finding is consistent with the above described observations for the O 1*s*. The fact that the suppression of the *s* signal in the perpendicular geometry is not complete, is a quite important detail that one has to keep in mind. In view of the very large transition metal 4*s* photoionization cross-section relative to that of the transition metal 3*d* and O 2*p* at these high photon energies, one should not assign all the spectral features in the valence band taken with the perpendicular geometry to the transition metal 3*d* or O 2*p*. The 4*s* signal does contribute as we can see from the second panel in Fig. 4.

5. Conclusions

We have investigated the efficiency of polarization dependent hard X-ray photoelectron spectroscopy (HAXPES) for solid state systems using NiO, ZnO and Cu_2O as reference materials. We have found that the polarization dependence is not as much as we have expected on the basis of atomic cross-section calculations, which we attribute to side-scattering processes suffered by the out going photoelectrons yielding an effective angular spread of about $\pm 18^\circ$. Yet, the polarization dependence is extremely large, we can achieve a 20:1 to 25:1 ratio for *s* orbitals, facilitating the quantitative determination of the contributions of the orbitals forming the valence band of solids. We have utilized this aspect to establish that the Ni 4*s* plays a substantial role in the chemical bonding of NiO. The strong polarization contrast also opens up the possibility to extend this type of experiments to the determination of the orientation of the occupied valence orbitals. One could envision, for example, to rotate a single crystal in a fixed light-polarization and analyzer geometry and measure the photoemission intensity of a particular valence band orbital, which then should reflect its charge density.

Acknowledgments

We would like to acknowledge R. Verbeni and C. Henriquet for their support at the ESRF and Lucie Hamdan for her skillful technical assistance. This work was supported by the Deutsche Forschungsgemeinschaft through SFB 608 and FOR 1346.

Appendix A. Supplementary data

Supplementary data associated with this article can be found, in the online version, at http://dx.doi.org/10.1016/j.elspec.2014.11.003.

References

[1] A. Sekiyama, J. Yamaguchi, A. Higashiya, M. Obara, H. Sugiyama, M.Y. Kimura, S. Suga, S. Imada, I.A. Nekrasov, M. Yabashi, K. Tamasaku, T. Ishikawa, The prominent 5d-orbital contribution to the conduction electrons in gold, New. J. Phys. 12 (4) (2010) 043045, http://dx.doi.org/10.1088/1367-2630/12/4/043045 http://stacks.iop.org/1367-2630/12/i=4/a=043045

[2] S. Ouardi, G.H. Fecher, X. Kozina, G. Stryganyuk, B. Balke, C. Felser, E. Ikenaga, T. Sugiyama, N. Kawamura, M. Suzuki, K. Kobayashi, Symmetry of valence states of heusler compounds explored by linear dichroism in hard-X-ray photoelectron spectroscopy, Phys. Rev. Lett. 107 (2011) 036402, http://dx.doi.org/10.1103/PhysRevLett.107.036402 http://link.aps.org/doi/10.1103/PhysRevLett.107.036402

[3] Y. Nakatsu, A. Sekiyama, S. Imada, Y. Okamoto, S. Niitaka, H. Takagi, A. Higashiya, M. Yabashi, K. Tamasaku, T. Ishikawa, S. Suga, Hard X-ray photoelectron spectroscopy of the metal-insulator transition in $LiRh_2O_4$, Phys. Rev. B 83 (2011) 115120, http://dx.doi.org/10.1103/PhysRevB.83.115120 http://link.aps.org/doi/10.1103/PhysRevB.83.115120

[4] S. Ouardi, G.H. Fecher, C. Felser, Bulk electronic structure studied by hard X-ray photoelectron spectroscopy of the valence band: The case of intermetallic compounds, J. Electron Spectrosc. Relat. Phenom. 190 (Part B (0)) (2013) 249–267, http://dx.doi.org/10.1016/j.elspec.2013.09.001 http://www.sciencedirect.com/science/article/pii/S0368204813001448

[5] See Supplementary Material at http://dx.doi.org/10.1016/j.elspec.2014.11.003 for the polarization study of ZnO and Cu_2O core levels.

[6] P. Torelli, M. Sacchi, G. Cautero, M. Cautero, B. Krastanov, P. Lacovig, P. Pittana, R. Sergo, R. Tommasini, A. Fondacaro, F. Offi, G. Paolicelli, G. Stefani, M. Grioni, R. Verbeni, G. Monaco, G. Panaccione, Experimental setup for high energy photoemission using synchrotron radiation, Rev. Sci. Instrum. 76 (2) (2005) 023909, http://dx.doi.org/10.1063/1.1852323 http://scitation.aip.org/content/aip/journal/rsi/76/2/10.1063/1.1852323

[7] J. Ghijsen, L.H. Tjeng, J. van Elp, H. Eskes, J. Westerink, G.A. Sawatzky, M.T. Czyzyk, Electronic structure of Cu_2O and CuO, Phys. Rev. B 38 (1988) 11322–11330, http://dx.doi.org/10.1103/PhysRevB.38.11322 http://link.aps.org/doi/10.1103/PhysRevB.38.11322

[8] M. Oku, H. Tokuda, K. Hirokawa, Final states after Ni2p photoemission in the nickel–oxygen system, J. Electron Spectrosc. Relat. Phenom. 53 (4) (1991) 201–211, http://dx.doi.org/10.1016/0368-2048(91)85039-V http://www.sciencedirect.com/science/article/pii/036820489185039V

[9] A.E. Bocquet, T. Mizokawa, T. Saitoh, H. Namatame, A. Fujimori, Electronic structure of 3d-transition-metal compounds by analysis of the 2p core-level photoemission spectra, Phys. Rev. B 46 (1992) 3771–3784, http://dx.doi.org/10.1103/PhysRevB.46.3771 http://link.aps.org/doi/10.1103/PhysRevB.46.3771

[10] S. Uhlenbrock, C. Scharfschwerdt, M. Neumann, G. Illing, H.J. Freund, The influence of defects on the Ni 2p and O 1s XPS of NiO, J. Phys. Condens. Matter. 4 (40) (1992) 7973 http://stacks.iop.org/0953-8984/4/i=40/a=009

[11] L. Sangaletti, L.E. Depero, F. Parmigiani, On the non-local screening mechanisms in the 2p photoelectron spectra of NiO and La_2NiO_4, Solid State Commun. 103 (7) (1997) 421–424, http://dx.doi.org/10.1016/S0038-1098(97)00185-3 http://wwwsciencedirectcom/science/article/pii/S0038109897001853

[12] S. Altieri, L.H. Tjeng, A. Tanaka, G.A. Sawatzky, Core-level X-ray photoemission on NiO in the impurity limit, Phys. Rev. B 61 (2000) 13403–13409, http://dx.doi.org/10.1103/PhysRevB.61.13403 http://link.aps.org/doi/10.1103/PhysRevB.61.13403

[13] M. Taguchi, M. Matsunami, Y. Ishida, R. Eguchi, A. Chainani, Y. Takata, M. Yabashi, K. Tamasaku, Y. Nishino, T. Ishikawa, Y. Senba, H. Ohashi, S. Shin, Revisiting the valence-band and core-level photoemission spectra of NiO, Phys. Rev. Lett. 100 (2008) 206401, http://dx.doi.org/10.1103/PhysRevLett.100.206401 http://link.aps.org/doi/10.1103/PhysRevLett.100.206401

[14] M.B. Trzhaskovskaya, V.I. Nefedov, V.G. Yarzhemsky, Photoelectron angular distribution parameters for elements $Z=1$ to $Z=54$ in the photoelectron energy range 100–5000 eV, Atom. Data Nucl. Data 77 (1) (2001) 97–159, http://dx.doi.org/10.1006/adnd.2000.0849 http://www.sciencedirect.com/science/article/pii/S0092640X00908490

[15] M.B. Trzhaskovskaya, V.K. Nikulin, V.I. Nefedov, V.G. Yarzhemsky, Non-dipole second order parameters of the photoelectron angular distribution for elements $Z=1--100$ in the photoelectron energy range 1–10 keV, Atom. Data Nucl. Data 92 (2) (2006) 245–304, http://dx.doi.org/10.1016/j.adt.2005.12.002 http://www.sciencedirect.com/science/article/pii/S0092640X05000859

[16] P.S. Shaw, U. Arp, S.H. Southworth, Measuring nondipolar asymmetries of photoelectron angular distributions, Phys. Rev. A 54 (1996) 1463–1472 http://link.aps.org/doi/10.1103/PhysRevA.54.1463

[17] F. Offi, A. Fondacaro, G. Paolicelli, A.D. Luisa, G. Stefani, Design and test of a lens system for a high energy and high resolution electron spectrometer, Nucl. Instrum Methods Phys. Res. A 550 (1-2) (2005) 454–466, http://dx.doi.org/10.1016/j.nima.2005.04.086 http://www.sciencedirect.com/science/article/pii/S0168900205012544

[18] A.X. Gray, C. Papp, S. Ueda, B. Balke, Y. Yamashita, L. Plucinski, J. Minr, J. Braun, E.R. Ylvisaker, C.M. Schneider, W.E. Pickett, H. Ebert, K. Kobayashi, C.S. Fadley, Probing bulk electronic structure with hard X-ray angle-resolved photoemission, Nat. Mater. 10 (10) (2011) 759–764, http://dx.doi.org/10.1038/nmat3089 http://dx.doi.org/10.1038/nmat3089

[19] M.A. Vicente Alvarez, H. Ascolani, G. Zampieri, Excitation of phonons and forward focusing in X-ray photoemission from the valence band, Phys. Rev. B 54 (1996) 14703–14712, http://dx.doi.org/10.1103/PhysRevB.54.14703 http://link.aps.org/doi/10.1103/PhysRevB.54.14703

[20] N.J. Shevchik, Disorder effects in angle-resolved photoelectron spectroscopy, Phys. Rev. B 16 (1977) 3428–3442, http://dx.doi.org/10.1103/PhysRevB.16.3428 http://link.aps.org/doi/10.1103/PhysRevB.16.3428]

[21] R.C. White, C.S. Fadley, M. Sagurton, Z. Hussain, Angle-resolved X-ray photoemission from the valence bands of tungsten with high angular resolution and temperature variation, Phys. Rev. B 34 (1986) 5226–5238, http://dx.doi.org/10.1103/PhysRevB.34.5226 http://link.aps.org/doi/10.1103/PhysRevB.34.5226

[22] In the derivation of the real experimental O 1*s* perpendicular vs. parallel intensity ratio, we have made use of the theoretical Ni 2*p*, Cu 2*p*, Zn 2*p* and Ni 3*d* intensity ratios to calibrate the intensities of the experimental perpendicular vs. parallel spectra. In principle a correction for the photoelectron scattering processes have to be made as well for these Ni 2*p*, Cu 2*p*, Zn 2*p* and Ni 3*d*. Using Eq. (3) instead of Eq. (2) and using $\alpha = 18^\circ$, we find that the Ni 2*p* ratio becomes 0.288 instead of 0.258 ($\beta = 0.98$) and the Ni 3*d* ratio 0.60 instead of 0.58 ($\beta = 0.39$). The corrections are thus of order.

[23] T.C. Koethe, J.C. Cezar, N.B. Brookes, Z. Hu, L.H. Tjeng, unpublished.

[24] J. van Elp, H. Eskes, P. Kuiper, G.A. Sawatzky, Electronic structure of Li-doped NiO, Phys. Rev. B 45 (1992) 1612–1622, http://dx.doi.org/10.1103/PhysRevB.45.1612 http://link.aps.org/doi/10.1103/PhysRevB.45.1612

[25] A. Fujimori, F. Minami, Valence-band photoemission and optical absorption in nickel compounds, Phys. Rev. B 30 (1984) 957–971, http://dx.doi.org/10.1103/PhysRevB.30.957 http://link.aps.org/doi/10.1103/PhysRevB.30.957

[26] G.A. Sawatzky, J.W. Allen, Magnitude and origin of the band gap in NiO, Phys. Rev. Lett. 53 (1984) 2339–2342, http://dx.doi.org/10.1103/PhysRevLett.53.2339 http://link.aps.org/doi/10.1103/PhysRevLett.53.2339
[27] K. Koepernik, H. Eschrig, Full-potential nonorthogonal local-orbital minimum-basis band-structure scheme, Phys. Rev. B 59 (1999) 1743–1757, http://dx.doi.org/10.1103/PhysRevB.59.1743 http://link.aps.org/doi/10.1103/PhysRevB.59.1743
[28] J.C. Woicik, E.J. Nelson, L. Kronik, M. Jain, J.R. Chelikowsky, D. Heskett, L.E. Berman, G.S. Herman, Hybridization and bond-orbital components in site-specific X-ray photoelectron spectra of rutile TiO_2, Phys. Rev. Lett. 89 (2002) 077401, http://dx.doi.org/10.1103/PhysRevLett.89.077401 http://link.aps.org/doi/10.1103/PhysRevLett.89.077401
[29] K. Kobayashi, Y. Takata, T. Yamamoto, J.-J. Kim, H. Makino, K. Tamasaku, M. Yabashi, D. Miwa, T. Ishikawa, S. Shin, T. Yao, Intrinsic valence band study of molecular-beam-epitaxy-grown GaAs and GaN by high-resolution hard X-ray photoemission spectroscopy, Jpn. J. Appl. Phys. 43 (8A) (2004) L1029 http://stacks.iop.org/1347-4065/43/i=8A/a=L1029
[30] G. Panaccione, G. Cautero, M. Cautero, A. Fondacaro, M. Grioni, P. Lacovig, G. Monaco, F. Offi, G. Paolicelli, M. Sacchi, N. Stojić, G. Stefani, R. Tommasini, P. Torelli, High-energy photoemission in silver: resolving d and sp contributions in valence band spectra, J. Phys. Condens. Matter 17 (17) (2005) 2671 http://stacks.iop.org/0953-8984/17/i=17/a=015
[31] D.J. Payne, R.G. Egdell, G. Paolicelli, F. Offi, G. Panaccione, P. Lacovig, G. Monaco, G. Vanko, A. Walsh, G.W. Watson, J. Guo, G. Beamson, P.-A. Glans, T. Learmonth, K.E. Smith, Nature of electronic states at the fermi level of metallic β-PbO_2 revealed by hard X-ray photoemission spectroscopy, Phys. Rev. B 75 (2007) 153102, http://dx.doi.org/10.1103/PhysRevB.75.153102 http://link.aps.org/doi/10.1103/PhysRevB.75.153102
[32] J.C. Woicik, M. Yekutiel, E.J. Nelson, N. Jacobson, P. Pfalzer, M. Klemm, S. Horn, L. Kronik, Chemical bonding and many-body effects in site-specific X-ray photoelectron spectra of corundum V_2O_3, Phys. Rev. B 76 (2007) 165101, doi:10.1103/PhysRevB.76.165101. URL http://link.aps.org/doi/10.1103/PhysRevB.76.165101.
[33] K. Kobayashi, Hard X-ray photoemission spectroscopy, Nucl. Instrum. Methods Phys. Res. A 601 (1–2) (2009) 32–47, http://dx.doi.org/10.1016/j.nima.2008.12.188, special issue in honour of Prof. Kai Siegbahn, http://www.sciencedirect.com/science/article/pii/S016890020802010X
[34] L.H. Tjeng, A.R. Vos, G.A. Sawatzky, Electronic structure of MgO studied by angle-resolved ultraviolet photoelectron spectroscopy, Surf. Sci. 235 (2–3) (1990) 269–279, http://dx.doi.org/10.1016/0039-6028(90)90802-F http://www.sciencedirect.com/science/article/pii/003960289090802F
[35] U. Schönberger, F. Aryasetiawan, Bulk and surface electronic structures of MgO, Phys. Rev. B 52 (1995) 8788–8793, http://dx.doi.org/10.1103/PhysRevB.52.8788 http://link.aps.org/doi/10.1103/PhysRevB.52.8788